Application of the Orthogonal Curvilinear Grid to FDTD Modeling of a Deflected Wind Turbine Blade

Franek, Ondrej

Published in:
Proceedings of the 2019 International Conference on Electromagnetics in Advanced Applications, ICEAA 2019

DOI (link to publication from Publisher):
10.1109/ICEAA.2019.8879203

Publication date:
2019

Document Version
Accepted author manuscript, peer reviewed version

Application of the Orthogonal Curvilinear Grid to FDTD Modeling of a Deflected Wind Turbine Blade

Ondřej Franek
Department of Electronic Systems, APMS Section
Aalborg University
Aalborg, Denmark
of@es.aau.dk

***Abstract*—Implementation of the orthogonal curvilinear grid in the finite-difference time-domain (FDTD) method to solve the problem of UWB propagation along a 58.7 m long wind turbine blade with various deflections is described. This approach is straightforward in that no rotation or bending of the blade model is needed, since it is the entire computational domain that is bent instead. The main benefit of this technique is that existing Cartesian FDTD code can be reused without any modification, as long as it allows inclusion of anisotropic materials.**

***Index Terms*—Ultrawideband propagation, FDTD**

I. Introduction

A wind turbine blade deflection sensing system utilizing ultrawideband (UWB) technology has recently been proposed [1], [2]. Employing a wireless link between an antenna near the blade tip and an antenna near the root, the system determines the amount of deflection (bending) of the blade by accurately measuring the time the UWB signal needs to travel between the two points. Detection of the pulse is accomplished by using a modified correlator trained on the rising edge of the UWB pulse.

Successful detection of the pulse requires sufficient signal-to-noise ratio and clean shape of the pulse. Since the tip antenna is placed inside the blade due to aerodynamic reasons and protection from lightning strikes, the signal has to pass the fiberglass shell of the blade and undergoes distortion due to multipath propagation components. In order to investigate the link budget for the detector and to optimize the position of the root antennas, we have used the finite-difference time-domain (FDTD) method [3] to simulate propagation of the UWB pulse along the 58.7m long blade.

We have found out that the worst case scenario occurs when the blade shape is straight or close to straight, and the UWB signal has to travel almost parallel to the blade surface. In this case, the received signal is generally weak and multipath distortion very strong. However, we also needed to investigate the scenario when the blade is deflected, because in that case some of the root antennas (if multiple root antennas are considered for better reliability) may end up in the blade radio shadow.

This work was supported by the Innovation Fund Denmark (Innovations-Fonden) project of *Intelligent Rotor for Wind Energy Cost Reduction* (project code 34-2013-2). The author also gratefully acknowledges the support from the Danish e-Infrastructure Cooperation (DeIC) for using the national HPC cluster *Abacus*.

It turned out that using the original FDTD method to simulate this kind of problem brings some difficulties due to the Cartesian grid. If the blade is deflected, then the root antenna and the tip antenna cannot be aligned with the grid at the same time, which can lead to substantial errors, especially for antennas based on thin substrates (in our case Vivaldi). Moreover, due to the bent shape of the deflected blade model, the FDTD computational domain has to be considerably larger, resulting in up to twice longer running times.

Several methods how to treat objects with curved surfaces in FDTD have been proposed in the past, these are summarized in [3]. Common disadvantage of the methods is that they require significant modifications to the FDTD code, sometimes even a complete rewrite of the code. More recently, a new formulation that allows implementation of curvilinear grid using standard rectangular FDTD update equations was proposed [4]. This work is based on an earlier finding [5] that a coordinate transformation in Maxwell's equations is equivalent to renormalizing the underlying material properties ϵ and μ. The advantage of this approach is that the original FDTD code can be reused without any modifications, only the material properties should be modified.

In the present paper, we describe the implementation of the orthogonal curvilinear grid in existing FDTD code to solve the problem of UWB propagation along a 58.7 m long wind turbine blade with various deflections. This problem is unique in that the coordinate system is varying along the blade body. The chosen approach has several benefits. Unlike previous simulations of a bent blade inside a rectangular FDTD domain, in the new implementation the entire computational domain is bent instead, so that the memory and CPU demands remain the same. As is pointed out in [4], the existing framework of the original FDTD code can be reused without modifications, because the curvature of the grid is created by changing the anisotropic material properties throughout the domain and not the underlying update equations. As such, the technique is applicable to any possible shape of the blade (or another body) without the necessity to generate a new model.

II. Simulation of a Deflected Blade

The deflection sensing system consists of a TX antenna inside the blade near the tip and two RX antennas outside near the blade root (Fig. 1). Successful detection of the UWB

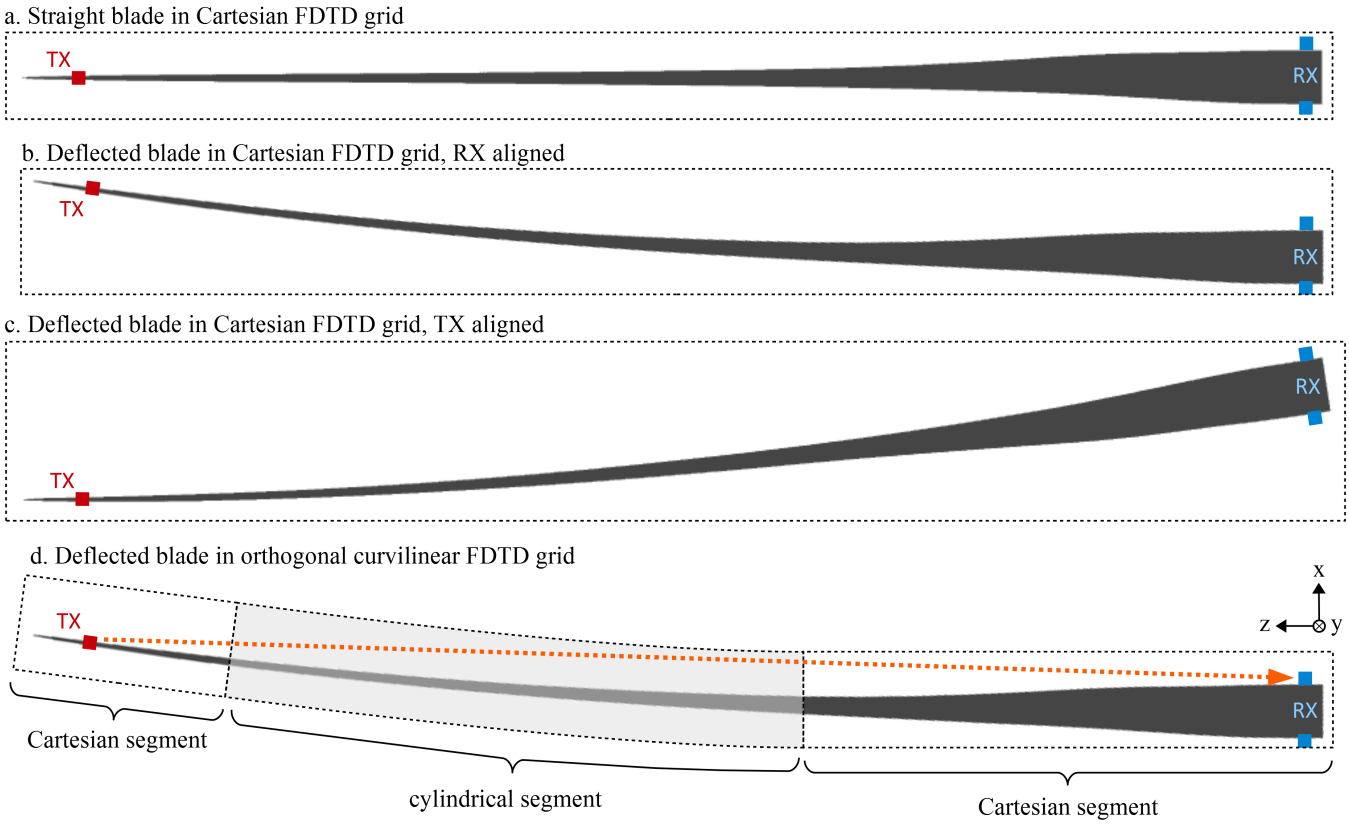

Fig. 1. Arrangement of the wind turbine blade in the FDTD computational domain: a. straight blade in Cartesian FDTD grid; b. deflected blade in Cartesian grid, RX aligned; c. deflected blade in Cartesian FDTD grid, TX aligned; d. deflected blade in orthogonal curvilinear FDTD grid. Dashed lines represent the FDTD computational domain boundaries, red squares positions of TX antennas, blue squares positions of RX antennas, the orange dotted line shows the propagation path and the grey area denotes the cylindrical segment of the FDTD grid.

pulse and accurate triangulation of the tip requires sufficient link budget that may change as the blade changes its shape when bending under the wind load. The purpose of the FDTD investigation is to find optimum positions for the RX antennas providing on average the best received signal for all possible deflections.

Figure 1 shows several cases of FDTD simulations of the 58.7 m long wind turbine blade. Simulation of a straight blade (Fig. 1a) is straightforward, as the TX and RX antennas are aligned with the grid. However, when the blade tip is deflected (Fig. 1b), the tip section is not aligned with the grid and would require excessive refinement of the mesh to accurately model the TX antenna. Since finding optimum positions of the RX antennas requires generally only knowing the field profiles at the root without the need to accurately model the RX antennas, we have chosen to rotate the entire blade in the grid and align the tip section with the TX antenna instead (Fig. 1c). This approach benefits from the aligned TX antenna, but it requires even larger computational domain due to the specific geometry of the blade.

The proposed solution is shown in Fig.1d. Since the blade is bent approximately in two thirds of its length (39.13 m), we have chosen to apply cylindrical coordinate system around this point in total length of 18 m, whereas the root and the tip section stay in the Cartesian coordinates where the antennas are aligned to the grid. There is also no need to modify the blade model, because its curvature changes naturally with the curvature of the coordinate system. The computational domain is only slightly larger than for the straight blade (Fig. 1a) to allow sufficient clearance for the direct wave (orange dotted line) next to the domain boundary.

III. FDTD in Orthogonal Curvilinear Grid

A. Update Equations

The FDTD update equations with time step Δt can be written in integral form as

$$E_x|^{n+1} = C_{\mathrm{a}x}E_x + (C_{\mathrm{b}x}/A_{Ex})\times (H_z l_{Hz} - H_z|_{j-1} l_{Hz}|_{j-1} - H_y l_{Hy} + H_y|_{k-1} l_{Hy}|_{k-1}) \quad (1a)$$

$$E_y|^{n+1} = C_{\mathrm{a}y}E_y + (C_{\mathrm{b}y}/A_{Ey})\times (H_x l_{Hx} - H_x|_{k-1} l_{Hx}|_{k-1} - H_z l_{Hz} + H_z|_{i-1} l_{Hz}|_{i-1}) \quad (1b)$$

$$E_z|^{n+1} = C_{\mathrm{a}z}E_z + (C_{\mathrm{b}z}/A_{Ez})\times (H_y l_{Hy} - H_y|_{i-1} l_{Hy}|_{i-1} - H_x l_{Hx} + H_x|_{j-1} l_{Hx}|_{j-1}) \quad (1c)$$

for the electric fields and

$$H_x = D_{\mathrm{a}x} H_x|^{n-1} - (D_{\mathrm{b}x}/A_{Hx})\times$$
$$(E_z|_{j+1} l_{Ez}|_{j+1} - E_z l_{Ez} - E_y|_{k+1} l_{Ey}|_{k+1} + E_y l_{Ey}) \quad (2a)$$
$$H_y = D_{\mathrm{a}y} H_y|^{n-1} - (D_{\mathrm{b}y}/A_{Hy})\times$$
$$(E_x|_{k+1} l_{Ex}|_{k+1} - E_x l_{Ex} - E_z|_{i+1} l_{Ez}|_{i+1} + E_z l_{Ez}) \quad (2b)$$
$$H_z = D_{\mathrm{a}z} H_z|^{n-1} - (D_{\mathrm{b}z}/A_{Hz})\times$$
$$(E_y|_{i+1} l_{Ey}|_{i+1} - E_y l_{Ey} - E_x|_{j+1} l_{Ex}|_{j+1} + E_x l_{Ex}) \quad (2c)$$

for the magnetic fields, where E_ξ and H_ξ are the electric and magnetic fields, respectively, in directions $\xi \in \{x, y, z\}$. The staggered fields are written in compact notation where each field has three subscripts for spatial position of the cell and one superscript for temporal position, as in $E_\xi|^n_{i,j,k} = E_\xi(i\Delta x, j\Delta y, k\Delta z, n\Delta t)$ and $H_\xi|^n_{i,j,k} = H_\xi(i\Delta x, j\Delta y, k\Delta z, n\Delta t)$, but the cell coordinates are omitted wherever no shift occurs. The update coefficients are also spatially dependent with the same compact notation

$$C_{\mathrm{a}\xi} = \frac{1 - \sigma_\xi \Delta t/2\epsilon_\xi}{1 + \sigma_\xi \Delta t/2\epsilon_\xi} \qquad C_{\mathrm{b}\xi} = \frac{\Delta t/\epsilon_\xi}{1 + \sigma_\xi \Delta t/2\epsilon_\xi} \quad (3)$$

$$D_{\mathrm{a}\xi} = \frac{1 - \sigma^*_\xi \Delta t/2\mu_\xi}{1 + \sigma^*_\xi \Delta t/2\mu_\xi} \qquad D_{\mathrm{b}\xi} = \frac{\Delta t/\mu_\xi}{1 + \sigma^*_\xi \Delta t/2\mu_\xi} \quad (4)$$

and the same applies to the underlying anisotropic material properties ϵ_ξ, μ_ξ, σ_ξ, and σ^*_ξ. Divisors $A_{E\xi}$ and $A_{H\xi}$ are cell face areas adjacent and normal to the respective fields E_ξ and H_ξ. Similarly, $l_{E\xi}$ and $l_{H\xi}$ are cell edge lengths adjacent and parallel to the respective fields E_ξ and H_ξ.

In case the coordinate system is Cartesian in the entire domain, the cell edge lengths become

$$l_{E\xi} = l_{H\xi} = \Delta\xi \quad (5)$$

where $\Delta\xi$ is the spatial step (cell size) along the particular coordinate direction ξ, and the cell face areas become

$$A_{Ex} = A_{Hx} = \Delta y \Delta z \quad (6a)$$
$$A_{Ey} = A_{Hy} = \Delta z \Delta x \quad (6b)$$
$$A_{Ez} = A_{Hz} = \Delta x \Delta y \quad (6c)$$

As a result, the update equations (1a)–(2c) reduce to the common Cartesian FDTD formulation.

Whenever the coordinate system needs to be curved, the $A_{E\xi}$, $A_{H\xi}$ and $l_{E\xi}$, $l_{H\xi}$ take different values corresponding to the curvature of the coordinates. In our case, as depicted in Fig. 1d, part of the computational domain is cylindrical, corresponding to bending of the blade in that area. Using the coordinates from Fig. 1d, the cell edge lengths become

$$l_{Ex} = l_{Hx} = \Delta x \quad (7a)$$
$$l_{Ey} = l_{Hy} = \Delta y \quad (7b)$$
$$l_{Ez} = l_{Hz} = \Delta z \cdot \alpha \quad (7c)$$

and the cell face areas

$$A_{Ex} = A_{Hx} = \Delta y \Delta z \cdot \alpha \quad (8a)$$
$$A_{Ey} = A_{Hy} = \Delta z \Delta x \cdot \alpha \quad (8b)$$
$$A_{Ez} = A_{Hz} = \Delta x \Delta y \quad (8c)$$

where

$$\alpha = 1 - \frac{x}{r} \quad (9)$$

is the curvature coefficient dependent on the coordinate x from the centerline of the blade and the radius of curvature $r = d/\delta$, where d is the length of the cylindrical coordinate segment along the blade and δ is the deflection angle.

Substituting (7a)–(8c) into (1a)–(2c) we obtain the curvilinear update equations, which differ from the Cartesian update equations in that some terms are multiplied by α. If we scale the z-oriented field components $E'_z = E_z\alpha$ and $H'_z = H_z\alpha$, we can get rid of the α coefficients in the curl terms on the right hand side, and the update equations will now have the Cartesian form where only the "b" set of update coefficients is modified:

$$C'_{\mathrm{b}x} = \frac{C_{\mathrm{b}x}}{\alpha} = \frac{\Delta t/\epsilon'_x}{1 + \sigma'_x \Delta t/2\epsilon'_x} \quad (10a)$$
$$C'_{\mathrm{b}y} = \frac{C_{\mathrm{b}y}}{\alpha} = \frac{\Delta t/\epsilon'_y}{1 + \sigma'_y \Delta t/2\epsilon'_y} \quad (10b)$$
$$C'_{\mathrm{b}z} = C_{\mathrm{b}z} \cdot \alpha = \frac{\Delta t/\epsilon'_z}{1 + \sigma'_z \Delta t/2\epsilon'_z} \quad (10c)$$

$$D'_{\mathrm{b}x} = \frac{D_{\mathrm{b}x}}{\alpha} = \frac{\Delta t/\mu'_x}{1 + \sigma^{*\prime}_x \Delta t/2\mu'_x} \quad (11a)$$
$$D'_{\mathrm{b}y} = \frac{D_{\mathrm{b}y}}{\alpha} = \frac{\Delta t/\mu'_y}{1 + \sigma^{*\prime}_y \Delta t/2\mu'_y} \quad (11b)$$
$$D'_{\mathrm{b}z} = D_{\mathrm{b}z} \cdot \alpha = \frac{\Delta t/\mu'_z}{1 + \sigma^{*\prime}_z \Delta t/2\mu'_z} \quad (11c)$$

These coefficient have also the same basic form as (3) and (4), only the material properties are modified

$$\epsilon'_x = \epsilon_x \cdot \alpha \qquad \sigma'_x = \sigma_x \cdot \alpha \quad (12a)$$
$$\epsilon'_y = \epsilon_y \cdot \alpha \qquad \sigma'_y = \sigma_y \cdot \alpha \quad (12b)$$
$$\epsilon'_z = \epsilon_z/\alpha \qquad \sigma'_z = \sigma_z/\alpha \quad (12c)$$

$$\mu'_x = \mu_x \cdot \alpha \qquad \sigma^{*\prime}_x = \sigma'_x \cdot \alpha \quad (13a)$$
$$\mu'_y = \mu_y \cdot \alpha \qquad \sigma^{*\prime}_y = \sigma'_y \cdot \alpha \quad (13b)$$
$$\mu'_z = \mu_z/\alpha \qquad \sigma^{*\prime}_z = \sigma'_z/\alpha \quad (13c)$$

The "a" set of update coefficients, $C_{\mathrm{a}\xi}$ and $D_{\mathrm{a}\xi}$, remains the same under the coordinate transformation.

B. Grid Boundaries

The computational domain is terminated in all six coordinate directions by perfectly matched layers (PML) to simulate free space around the blade. Implementation of the PML in cylindrical coordinates follows the same principle as described above, with the α coefficients incorporated into the dispersive anisotropic medium of the PML layers.

Boundaries between the Cartesian and the cylindrical grid feature slightly different α coefficients, since some cell edges

and faces are partially in the Cartesian and partially in the cylindrical grid. In particular:

$$A_{Ex}^{(\text{boundary})} = \frac{1}{2}\Delta y\Delta z + \frac{1}{2}\Delta y\Delta z \cdot \alpha = \Delta y\Delta z\frac{\alpha+1}{2} \quad (14)$$

$$A_{Ey}^{(\text{boundary})} = \frac{1}{2}\Delta z\Delta x + \frac{1}{2}\Delta z\Delta x \cdot \alpha = \Delta z\Delta x\frac{\alpha+1}{2} \quad (15)$$

$$l_{Hz}^{(\text{boundary})} = \frac{1}{2}\Delta z + \frac{1}{2}\Delta z \cdot \alpha = \Delta z\frac{\alpha+1}{2} \quad (16)$$

C. Stability Condition

Since the cylindrical coordinate system affects only one dimension of the cell, in our case the z-oriented, derivation of the new time step satisfying stability condition is straightforward

$$\Delta t \leq c^{-1}\left[\Delta x^{-2} + \Delta y^{-2} + \Delta z^{-2}(\min\alpha)^{-2}\right]^{(-1/2)} \quad (17)$$

Here, $c = 1/\sqrt{\epsilon_0\mu_0}$ is the propagation speed in vacuum and $\min\alpha$ stands for the minimum value of α in the grid. Furthermore, our blade simulation utilized cubical cells in the Cartesian grid, $\Delta x = \Delta y = \Delta z$, so the new time step could be expressed simply as

$$\Delta t^{(\text{new})} = \Delta t^{(\text{orig})}\left[\frac{2+(\min\alpha)^{-2}}{3}\right]^{(-1/2)} \quad (18)$$

IV. Results

The 58.7m long wind turbine blade has been modeled using cubical cells with edge length 5 mm. The tip antenna was placed at distance 56.45 m from the blade root and excited with Gauss-sine pulse with bandwidth 3–5 GHz.

Figure 2 shows two E_x field profiles for straight blade (top) and deflected blade with angle $\delta = 8.6°$ (bottom). The fields are taken as peak values of the time-domain pulses at the z-normal plane 2 m from the blade root. The TX antenna placed inside the blade has its beam radiating towards the root, but slightly tilted towards the x direction. When the blade is deflected, the beam starts radiating towards the root and the field levels (and, correspondingly, the signal-to-noise ratio) are elevated, both outside and, after penetrating the blade shell, also inside. The multipath effects due to reflections from the blade surface are clearly visible.

V. Conclusion

Using the FDTD method with orthogonal curvilinear grid to simulate UWB propagation along deflected wind turbine blade has many benefits. Since it is only the material properties that describe the curvature of the coordinate system, it is possible to reuse the Cartesian FDTD code without any modifications. The only condition is that the existing code must allow inclusion of anisotropic materials. Finally, the anisotropic material formulation also makes it simple to determine the upper limit of the time step for numerical stability. The method was demonstrated by assuming cylindrical coordinate system on a segment of the computational domain and simplified modeling of the deflection. However, arbitrary curvature of the blade is possible with this technique.

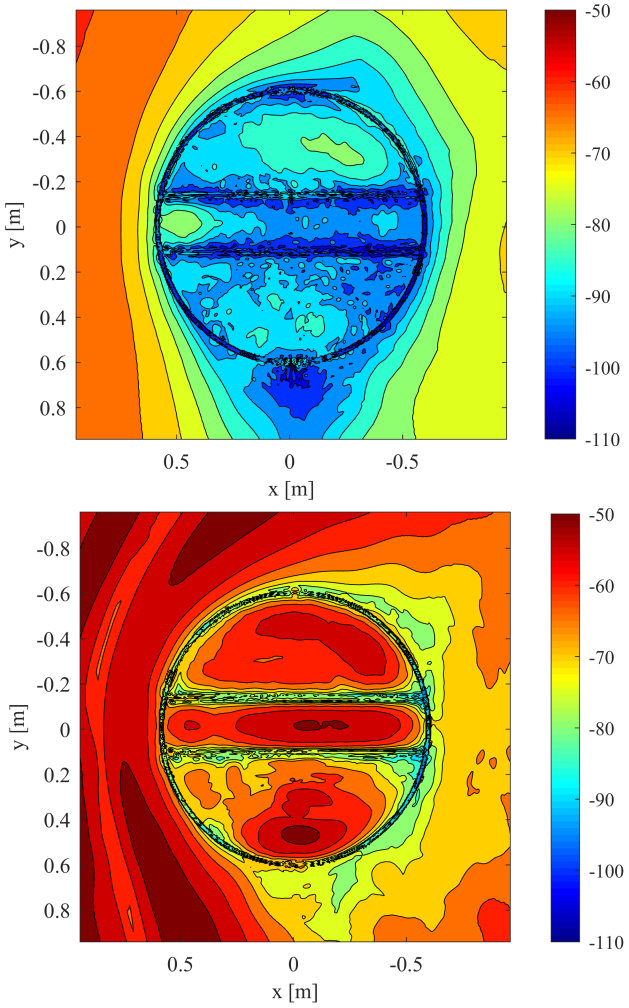

Fig. 2. Electric field E_x profiles in dBV/m at distance $z = 2$ m from the blade root with the TX antenna near the blade tip. Top: straight blade; Bottom: $\delta = 8.6°$ deflection of the tip. The fiberglass structure of the blade is identifiable in the cross section.

Acknowledgment

The author would like to thank Peter Bæk and Claus Byskov at LM Wind Power for providing the voxel model of the wind turbine blade used in the numerical experiment.

References

[1] S. Zhang, T. L. Jensen, O. Franek, P. C. Eggers, K. Olesen, C. Byskov, and G. F. Pedersen, "UWB wind turbine blade deflection sensing for wind energy cost reduction," *Sensors*, vol. 15, no. 8, pp. 19 768–19 782, 2015.

[2] S. Zhang, T. L. Jensen, O. Franek, P. C. Eggers, C. Byskov, and G. F. Pedersen, "Investigation of a UWB wind turbine blade deflection sensing system with a tip antenna inside a blade," *IEEE Sensors Journal*, vol. 16, no. 22, pp. 7892–7902, 2016.

[3] A. Taflove and S. C. Hagness, *Computational electrodynamics: The Finite-Difference Time-Domain Method*, 3rd ed. Boston: Artech house, 2005.

[4] R. T. Lee, J. G. Maloney, B. N. Baker, and D. W. Landgren, "FDTD in curvilinear coordinates using a rectangular FDTD formulation," in *2011 IEEE International Symposium on Antennas and Propagation (APS-URSI)*. IEEE, 2011, pp. 2326–2329.

[5] A. Ward and J. B. Pendry, "Refraction and geometry in Maxwell's equations," *Journal of Modern Optics*, vol. 43, no. 4, pp. 773–793, 1996.